Article

Developmental Cell

The Ecdysone Receptor Coactivator Taiman Links Yorkie to Transcriptional Control of Germline Stem Cell Factors in Somatic Tissue

Graphical Abstract

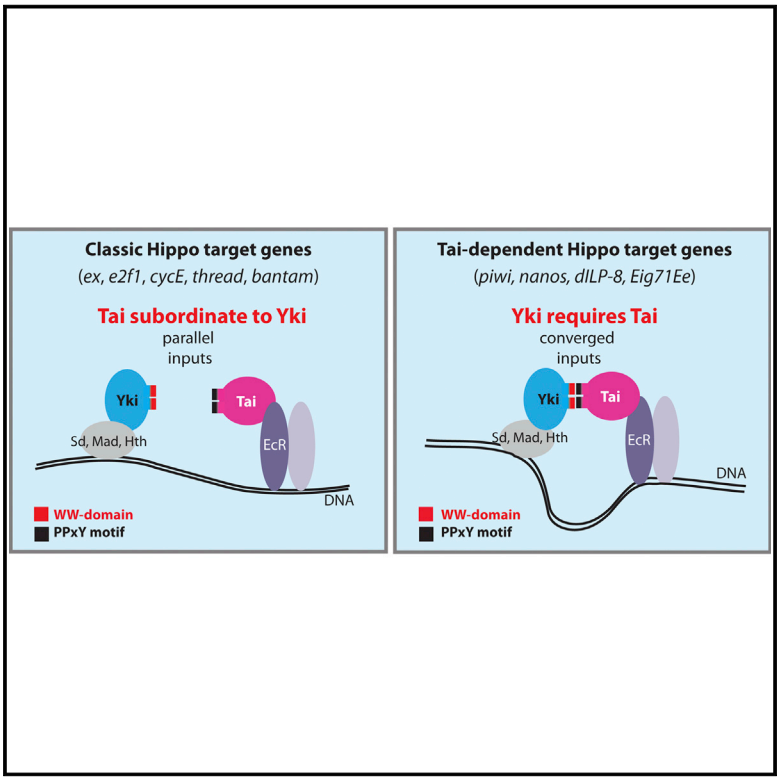

Highlights

- The *Drosophila* EcR coactivator Tai binds the Hippo pathway coactivator Yki
- Tai modulates expression of classic Yki target genes in developing imaginal discs
- Tai's role in Yki-driven hyperplasia is independent of classic Yki target genes
- Tai links hyperactive Yki to expression of germline mRNAs in disc cells

Authors

Can Zhang, Brian S. Robinson, Wenjian Xu, ..., Peng Jin, Alexey Veraksa, Kenneth H. Moberg

Correspondence

kmoberg@emory.edu

In Brief

Zhang and Robinson et al. define an interaction between the Hippo pathway component Yorkie and the ecdysone receptor transcriptional coactivator Taiman. This interaction links Yorkie to mRNAs of germline stem cell factors Piwi and Nanos, identifying them as required elements of a Hippo-repressed growth program in somatic disc cells.

Zhang et al., 2015, Developmental Cell *34*, 168–180
July 27, 2015
http://dx.doi.org/10.1016/j.devcel.2015.05.010

CellPress

CellPress

Developmental Cell
Article

The Ecdysone Receptor Coactivator Taiman Links Yorkie to Transcriptional Control of Germline Stem Cell Factors in Somatic Tissue

Can Zhang,[1,6] Brian S. Robinson,[1,2,6] Wenjian Xu,[5] Liu Yang,[5] Bing Yao,[3] Heya Zhao,[5] Phil K. Byun,[1,4] Peng Jin,[3] Alexey Veraksa,[5] and Kenneth H. Moberg[1,*]

[1]Department of Cell Biology
[2]Department of Pathology & Laboratory Medicine
[3]Department of Human Genetics
[4]Graduate Program in Genetics and Molecular Biology
Emory University School of Medicine, Atlanta, GA 30322, USA
[5]Department of Biology, University of Massachusetts Boston, Boston, MA 02125, USA
[6]Co-first author
*Correspondence: kmoberg@emory.edu
http://dx.doi.org/10.1016/j.devcel.2015.05.010

SUMMARY

The Hippo pathway is a conserved signaling cascade that modulates tissue growth. Although its core elements are well defined, factors modulating Hippo transcriptional outputs remain elusive. Here we show that components of the steroid-responsive ecdysone (Ec) pathway modulate Hippo transcriptional effects in imaginal disc cells. The Ec receptor coactivator Taiman (Tai) interacts with the Hippo transcriptional coactivator Yorkie (Yki) and promotes expression of canonical Yki-responsive genes. Tai enhances Yki-driven growth, while Tai loss, or a form of Tai unable to bind Yki, suppresses Yki-driven tissue growth. This growth suppression is not correlated with impaired induction of canonical Hippo-responsive genes but with suppression of a distinct pro-growth program of Yki-induced/Tai-dependent genes, including the germline stem cell factors *nanos* and *piwi*. These data reveal Hippo/Ec pathway crosstalk in the form a Yki-Tai complex that collaboratively induces germline genes as part of a transcriptional program that is normally repressed in developing somatic epithelia.

INTRODUCTION

Most metazoan organisms grow during embryogenesis and a subsequent juvenile stage, which in vertebrates coincides with hormone-driven sexual maturation. The extent of growth is determined in part by extracellular signals in the form of locally acting morphogens and systemic growth factors. In the fruit fly *Drosophila melanogaster*, these local and systemic factors act in concert with nutrient-sensing pathways to regulate growth of pockets of diploid epithelial cells termed imaginal discs that grow during embryonic and larval stages and are reshaped during pupation into adult organs (Fristrom, 1970; Nijhout et al., 2014). The ecdysteroid 20-hydroxyecdysone (20E), the hydroxylated metabolite of ecdysone (Ec), triggers pupal metamorphosis and accompanying histolysis of most larval tissues (Riddiford, 1993) by binding a heterodimer of Ec receptor (EcR) and Ultraspiracle (Usp), which are homologs of vertebrate nuclear hormone receptors (Koelle et al., 1991; Thomas et al., 1993; Yao et al., 1992). The EcR-Usp heterodimer activates or represses gene transcription depending on bound cofactors (Hu et al., 2003; Tsai et al., 1999). 20E binding stimulates release of EcR-associated repressors such as Smrter (Tsai et al., 1999) and recruitment of coactivators that support expression of Ec-response genes (Bayer et al., 1996; DiBello et al., 1991).

In addition to stimulating larval instars and pupal metamorphosis, EcR regulates growth of larval imaginal tissue via autonomous and non-cell autonomous mechanisms. EcR activity in the larval fat body (FB) systemically suppresses growth by lowering production of insulin-like peptides (dILPs) by neuroendocrine cells (Boulan et al., 2013; Delanoue et al., 2010). Genetic reduction of EcR in the FB thus elevates insulin-like growth factor (IGF) activity in the periphery, leading to increased growth (Delanoue et al., 2010). In contrast, imaginal disc cells lacking EcR or the Ecdysoneless protein (Ecd), which is cell autonomously required for production of low levels of Ec, proliferate at reduced rates relative to normal cells (Brennan et al., 1998; Delanoue et al., 2010; Gaziova et al., 2004; Henrich et al., 1987). Ecdysteroids have been linked to expression of genes involved in cell division and growth (Ghbeish and McKeown, 2002; Ghbeish et al., 2001; Mitchell et al., 2008; Nijhout and Grunert, 2002). However, cell-autonomous mediators of EcR proliferative effects and the degree to which the EcR pathway engages in crosstalk with other proliferative pathways are not well defined. A better understanding of this aspect of EcR biology could illuminate mechanisms that modulate developmental growth and are affected in diseases of altered nuclear receptor signaling.

The transcriptional coactivator protein Taiman (Tai) binds EcR and supports EcR-mediated effects in the ovary and border cells (Bai et al., 2000; Jang et al., 2009; König et al., 2011). Tai is a homolog of the vertebrate family of p160 nuclear receptor coactivators (NCOA1,2,3, also known as steroid receptor coactivator

[SRC]-1,2,3) and has highest sequence homology to NCOA3, also termed amplified in breast cancer-1 (AIB-1) due to its overexpression in breast cancers (reviewed in Yan et al., 2006). The Tai protein contains N-terminal basic-helix-loop-helix (bHLH) and PAS (Per-Arnt-Sim) domains, a centrally located receptor interaction domain (RID) containing a pair of Leucine-x-x-Leucine-Leucine (LxxLL) motifs that interact with EcR, and a C-terminal glutamine-rich transcriptional activation domain (TAD) (Bai et al., 2000). Tai has a well-defined role in invasive behavior of border cells (Bai et al., 2000; Jang et al., 2009) and a proposed pro-growth role in epithelial cells (Turkel et al., 2013), but its normal role in disc development is less clear.

Here we define a role for Tai in autonomous control of imaginal disc growth in a complex with Yorkie (Yki), the transcriptional co-activator of the Hippo pathway (reviewed in Staley and Irvine, 2012). The ability of Tai to promote growth correlates with a Tai-Yki complex mediated by a pair of PPxY (proline-proline-x-tyrosine) motifs in the Tai TAD and two WW (tryptophan-tryptophan) domains in Yki. Tai enhances the effect of Yki on disc growth, while a mutant form of Tai unable to bind Yki suppresses Yki-driven growth. At a transcriptional level, Tai regulates expression of the canonical Yki-target genes *expanded*, *diap-1*, *e2f1*, and *bantam* and can associate with a segment of the *bantam* promoter that also interacts with EcR and Yki (modEncode Consortium et al., 2010; Oh and Irvine, 2011). EcR is required for Tai-driven activation of *expanded* and *diap-1*, further supporting the hypothesis that Tai and Yki co-regulate a transcriptional program in disc cells. However, the Tai dependence of Yki-driven overgrowth is not reflected by effects on canonical Yki transcriptional targets but rather by failure to induce a distinct group of Yki-inducible/Tai-dependent mRNAs identified by a transcriptome-wide RNA analysis. Two of these mRNAs, *nanos* and *piwi*, encode RNA binding proteins that are highly expressed in the germline, where they support self-renewing division of germline stem cells (GSCs) (reviewed in Losick et al., 2011; Ross et al., 2014). Yki requires Tai to induce *nanos* and *piwi* in disc cells, and individual depletion of either GSC factor partially suppresses Yki-driven overgrowth. Collectively, these findings identify Tai as a key regulator of Yki activity in vivo and provide evidence that Tai-dependent induction of factors associated with GSC renewal is one element of a transcriptional program normally repressed by the Hippo pathway in developing somatic epithelia.

RESULTS

Tai Supports Tissue Growth

In view of the role of Tai as an EcR coactivator, alleles of the *taiman* (*tai*) gene were examined for effects on tissue growth. Null *tai* alleles are lethal (Bai et al., 2000; König et al., 2011), but two hypomorphic alleles (tai^{k15101} and tai^{k05809}) in *trans* to an uncovering genomic deficiency (*ED678*) yield adults that are small and show an approximate 20% reduction in adult wing size relative to controls (Figures 1A and 1B). Tai protein is detected in third instar larval (L3) wing disc cells and manipulating Tai levels in these cells with a *UAS-tai* transgene (Bai et al., 2000) or a *tai* RNAi line (TRiP *HM05182*; hereafter referred to as tai^{IR}) (Figures S1A and S1B) produces growth effects restricted to the site of expression (Figures 1C–1F). Expression of the *UAS-tai* transgene with the *engrailed-Gal4* (*en-Gal4*) posterior (P) compartment driver (*en>tai*) expands the P domain of L3 wing discs, particularly in the pouch (Figure 1D). Reciprocal depletion of Tai (*en>*tai^{IR}) shrinks the P domain without significantly altering the size of the Cubitus interruptus (Ci)-positive anterior (A) domain (Figure 1E). Quantitation of relative A and P domain sizes among *en>tai* and *en>*tai^{IR} L3 discs confirms the autonomous effect of Tai gain or loss (Figure 1F). Clonal analysis using the *Actin>CD2>Gal4* "Flp-out" technique (Pignoni and Zipursky, 1997) confirms that Tai-expressing clones grow larger than age-matched control clones (Figure 1G). The *en>tai* and *en>*tai^{IR} genotypes are each lethal in the pupal phase (data not shown), precluding analysis of adult phenotypes. However, adult animals expressing the tai^{IR} transgene from the pouch driver *MS1096-Gal4* have significantly smaller wings than WT counterparts (Figures 1H and 1I). Morphologically, *tai*-expressing wing tissue is excessively folded (Figures S1C and S1D) with evidence of increased S-phase entry (Figure 1J). *en>tai* P cells also express elevated levels of the Broad Z3 protein (Figure S1E), which is induced in cultured discs by 20E (Bayer et al., 1996). In sum, these data are consistent with Tai inducing Ec-responsive genes and proliferative genes in L3 wing cells.

Tai Interacts with Yki

Tai pro-growth activity could be based on its ability to interact with proteins that act within established proliferative pathways. Proteomic analyses in cultured cells identified the Hippo pathway component and pro-growth transcriptional coactivator Yki as a candidate Tai-interacting protein (A.V. and K.H.M., unpublished data; Kwon et al., 2013). A search for motifs within Tai that could mediate Yki-binding revealed two PPxY (proline-proline-x-tyrosine) motifs located within the C-terminal TAD (P_{1432}PAY and P_{1476}PMY) (Figure 2A). Closely paired PPxY motifs in other Hippo pathway components bind WW domains present in Yki (Badouel et al., 2009; Gilbert et al., 2011; Oh et al., 2009; Salah and Aqeilan, 2011). Co-immunoprecipitation of tagged forms of Tai and Yki confirms that each protein readily associates with the other in cultured *Drosophila* S2 cells (Figure 2B, lane 2, and Figure 2C, lane 5). Tyr-to-Ala (tyrosine-to-alanine) mutations in key tyrosine residues within one or both of the Yki WW domains (Yki^{Y281A}, Yki^{Y350A}, or $Yki^{\Delta WW2}$) block interaction with Tai (Figure 2B). Yki is not co-precipitated with versions of Tai carrying Tyr-to-Ala mutations in one or both of the PPxY motifs ($PPxA^{1}$, $PPxA^{2}$, or both $PPxA^{1,2}$) (Figure 2C). Consistent with these S2 cell data, endogenous Tai co-purifies with Yki-GFP expressed in 0- to 16-hr embryos (*daGal4,UAS-Yki-GFP*), as indicated by the recovery of multiple Tai peptides in mass spectrometry analysis, with the highest possible confidence SAINT score of 1 ("significance analysis of interactome"; Choi et al., 2011) (Figure S2A). In aggregate, these data indicate that paired PPxY motifs in the Tai TAD can facilitate interaction with the WW domains in Yki.

The presence of Yki and EcR-interaction motifs in the Tai protein suggests that it might be capable of forming a physical complex with both proteins. To assess whether an EcR-Tai-Yki complex can be assembled in cells, epitope-tagged EcR was expressed together with tagged forms of Tai and Yki in S2 cells. Precipitation via the V5-tag on Yki can recover EcR, but only in the presence of co-expressed Tai (Figure 2D, lane 1 versus

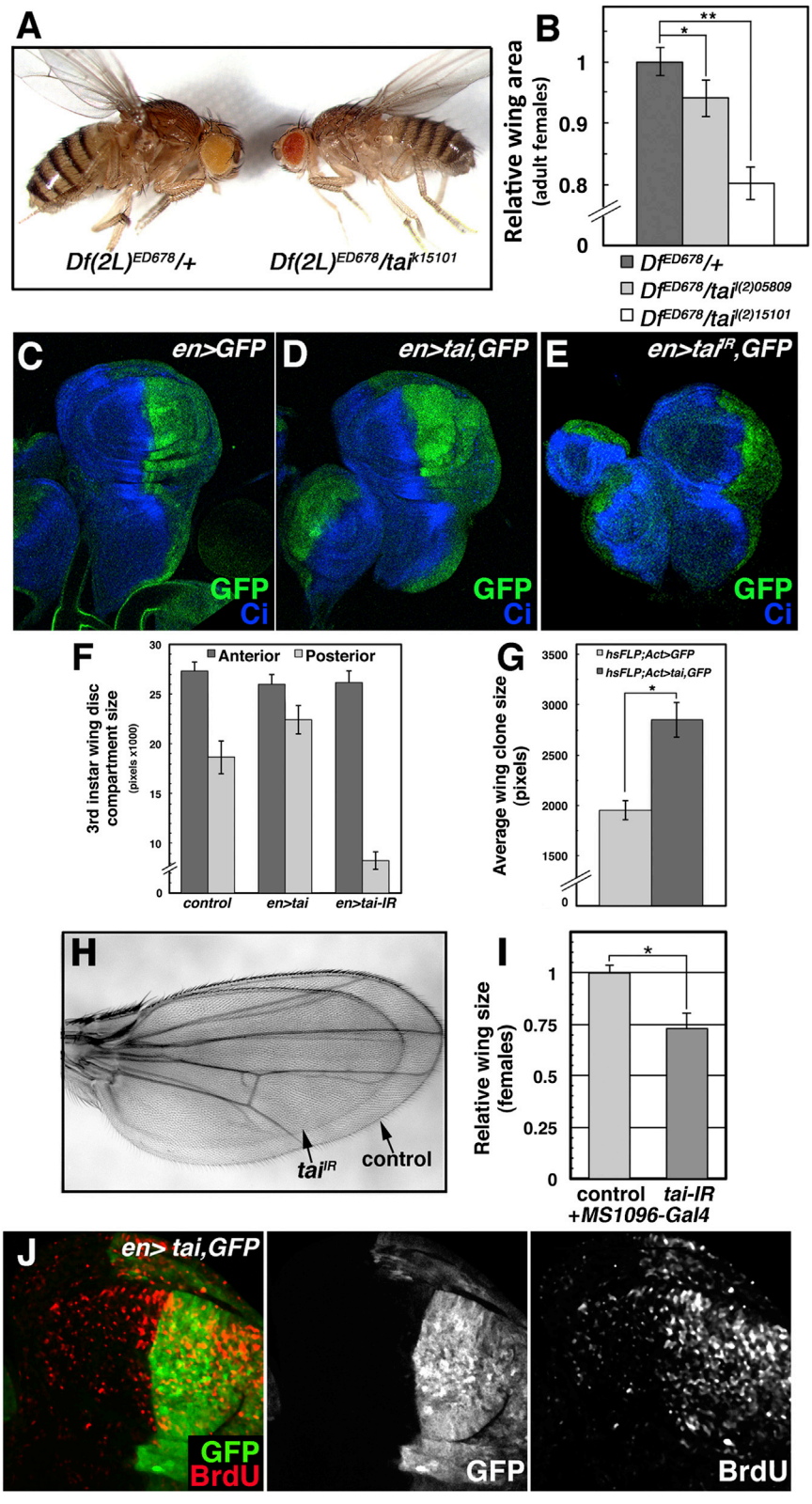

Figure 1. *tai* Supports Organism Growth

(A) Paired control (*Df(2L)ED678*/+) and *tai* mutant (*Df(2L)ED678/tai^{k15101}*) adult females.

(B) Quantitation of adult female wing size among the indicated genotypes (SEMs are shown; n = 12 for *Df(2L)ED678*/+ and *Df(2L)ED678/tai^{k05809}*, n = 14 for *Df(2L)ED678/tai^{k15101}*; *p = 2.9e-2, **p = 5.3e-6).

(C–E) L3 wing discs of the indicated genotypes expressing GFP (green) and immunostained with anti-Ci (blue) to mark the anterior (A, blue) and posterior (P, green) domains. Unless otherwise noted, the *UAS-tai^{IR}* TRiP transgene *HM05182* is used in Tai-knockdown experiments.

(F) Relative A (dark gray) versus P (light gray) areas among L3 wing discs of the genotypes shown in (C)–(E) (SEMs are shown; n = 12 for *en>+*, n = 15 for *en>tai*, n = 10 for *en>tai^{IR}*; p = 3.8e-2 and p = 4.4e-6, respectively, for *en>tai* and *en>tai-IR* relative to *en>+*).

(G) Average 2D size of 48-hr Actin-Gal4 "Flp out" clones expressing *GFP* (light gray) or *GFP* and *tai* (dark gray) (SEMs are shown; n = 79 for *UAS-GFP*, n = 112 for *UAS-GFP,tai*; *p = 2.5e-2).

(H and I) Overlay and quantitation of wing size among control adult female and Tai-depleted females (*tai^{IR}*) using the *MS1096* driver (SEMs are shown in I; n = 11 for *MS1096>+* and n = 13 for *MS1096>tai^{IR}*; *p = 2.2e-12).

(J) Confocal image of an *en>tai,GFP* L3 wing disc analyzed by BrdU incorporation (red) shows elevated S-phase entry in the P domain (green).

A Form of Tai that Cannot Bind Yki Antagonizes Yki-Stimulated Growth

The physical interaction between Tai and Yki points to potential cooperativity between the two proteins. Tai transgenes were expressed alone or in combination with a transgene encoding a hyperactive form of Yki using a *GMR-Gal4* driver (*GMR>yki^{S168A}*) active in the larval and pupal eye (Hay et al., 1997). Expression of WT Tai (*tai^{wt}*) with *GMR-Gal4* moderately expands adult eye size and enhances eye overgrowth in *GMR>yki^{S168A}* adults (Figures 3A, 3B, S2B, and S2D versus Figures S2C and S2E). Tai depletion with the *tai^{IR}* transgene leads to low adult survival in the *GMR>yki^{S168A}* background (data not shown), but shrinks adult head and eye size in both WT and *GMR>yki^{S168A}* backgrounds (Figures 3C, S2H, and S2I). *ey-FLP*-mediated production of clones homozygous for the null allele *tai^{61G1}* (Bai et al., 2000) in the *GMR>yki^{S168A}* background also reduced adult head and eye size (Figure S2K). Suppression of *GMR>yki^{S168A}* by *tai* alleles is not as complete as that provided by depletion of Yki-interacting transcription factor Scalloped

lane 4), indicating that Tai is required to detect an Yki-EcR complex. Thus, Tai is capable of bridging an interaction between these transcriptional regulators in cells.

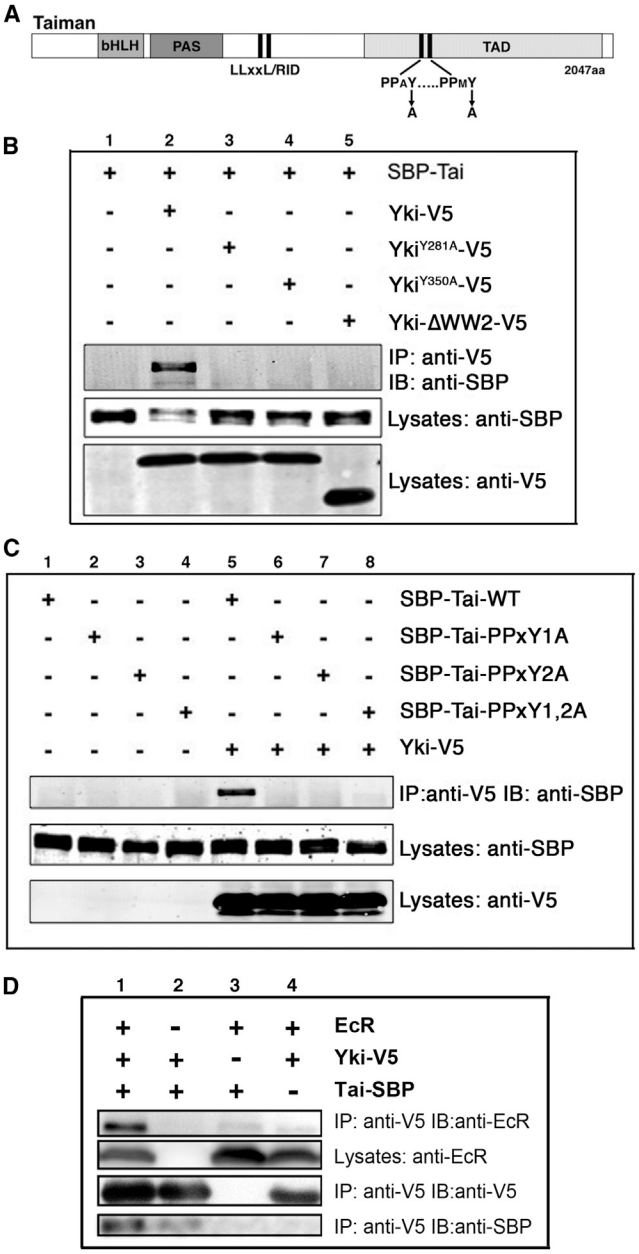

Figure 2. Tai Interacts Physically with Yki and EcR

(A) Tai domain structure. Approximate locations of the two PPxY motifs and their Y-to-A mutant forms are indicated.

(B) Co-immunoprecipitation (coIP) analysis of S2 cell lysates expressing SBP-tagged Tai and V5-tagged WT Yki or mutant forms of Yki with Y-to-A mutations in either (Y281 or Y350) or both (ΔWW2) WW domains.

(C) CoIP analysis of S2 cell lysates expressing V5-Yki with SBP-tagged WT Tai or with mutant forms of Tai with Y-to-A mutations in either (PPxY1A or PPxY2A) or both (PPxY1,2A) PPxY motifs.

(D) Immunoprecipitation of EcR with Yki from S2 cell lysates expressing SBP-Tai, V5-Yki, and EcR. Note the failure to recover EcR from anti-V5-Yki precipitates when Tai is not co-expressed (lane 4).

(Sd) (Figure S2J), implying that Tai enhances rather than mediates Yki transcriptional activity in vivo. Consistent with this hypothesis, a sd^{IR} transgene strongly suppresses the combined oncogenic effect of co-expressing Yki and Tai in the developing eye (Figure S3A).

The location of the PPxY sites in the Tai TAD implies that a physical interaction with Yki may be part of the mechanism by which Tai affects transcription of genes involved in imaginal disc development. *GMR-Gal4* directed expression of a *UAS-tai*^{PPxA1,2} transgene (Ala substitutions at Tyr_{1435} and Tyr_{1479}), which is expressed to equivalent levels as the *UAS-tai*^{WT} transgene in larval wing disc cells (Figure S3B), shrinks the size of adult eyes (Figures S2B and S2F), and suppresses overgrowth of *GMR>yki*^{S168A} adult eyes (Figures 3D and S2G). Larval *GMR>yki*^{S168A} eye discs show precocious entry into the synthesis (S) phase of the cell division cycle and enlargement of the sheet of epithelial tissue posterior to the MF (see bracketed areas in Figures 3E–3H). Relative to *GMR-yki*^{S168A} alone, co-expression of *yki*^{S168A} with *tai*^{WT} causes large folds of excess tissue and enhanced S-phase entry among cells behind the MF (Figures 3F and 3G). *GMR>yki*^{S168A}*+tai* discs also show greater spacing between adjacent F-actin enriched apical tufts of photoreceptor clusters behind the MF relative to *GMR>yki*^{S168A} (Figures 3J and 3K). This combined effect of WT Tai and Yki on cell division and photoreceptor spacing is reversed when Yki is co-expressed with Tai^{PPxA1,2}. The pattern of S-phase entry in *GMR>yki*^{S168A}*+tai*^{PPxA1,2} discs resembles that in *GMR-Gal4* control discs, and the distance between apical photoreceptor tufts in *GMR>yki*^{S168A}*+tai*^{PPxA} eye discs is nearer to WT dimensions (Figures 3H and 3L). Thus, the ability of Tai and Yki to cooperatively induce tissue growth is based on a PPxY:WW module through which these proteins can interact, and amino acid substitutions in Tai that prevent Yki-binding convert Tai into antigrowth factor that acts in a dominant-negative fashion to block Yki-driven tissue growth.

Endogenous Tai Supports Yki-Driven Tissue Growth

To assess whether *tai* contributes to growth of disc cells with inactive Hippo signaling, null alleles of *tai* and the Yki-inhibitor *expanded* (*ex*) were used in conjunction with tissue-specific *Flp* transgenes to generate disc cells lacking one or both genes (Figures 3M–3S). Consistent with the systemic effect of *tai* alleles on wing and body size (Figure 1), *tai* mosaic adult wings generated with the *Ultrabithorax (Ubx)-Flp* transgene are reduced in size relative to control organs, while *ex* mosaic wings are enlarged due to Yki hyperactivity (Hamaratoglu et al., 2006). Loss of Tai partially suppresses the *ex* phenotype such that *ex,tai* mosaic wings are smaller than *ex* mosaic wings (Figures 3M and 3N). *ex,tai* clones in L3 discs also appear smaller than age-matched *ex* clones (Figures 3O and 3P), and direct analysis of clone:twinspot ratios confirms that *tai* loss can suppress excess growth of *ex* mutant larval disc cells (Figures 3Q–3S). *tai* loss does not correct the characteristic broadened shape of *ex* mosaic wings, indicative of a Tai-independent mechanism supporting this aspect of the *ex* mutant wing phenotype. *tai* loss also shrinks adult head and eye size and suppresses head and eye overgrowth produced by clones of *ex* mutant cells, although the strength of the suppressive effect of *tai* on *ex* phenotypes is less than that observed in wings (Figures S4A–S4E). Genetic interactions are also observed between *tai* alleles and the Hippo component Crumbs, an apical membrane protein that couples apicobasal polarity cues to nuclear Yki activity

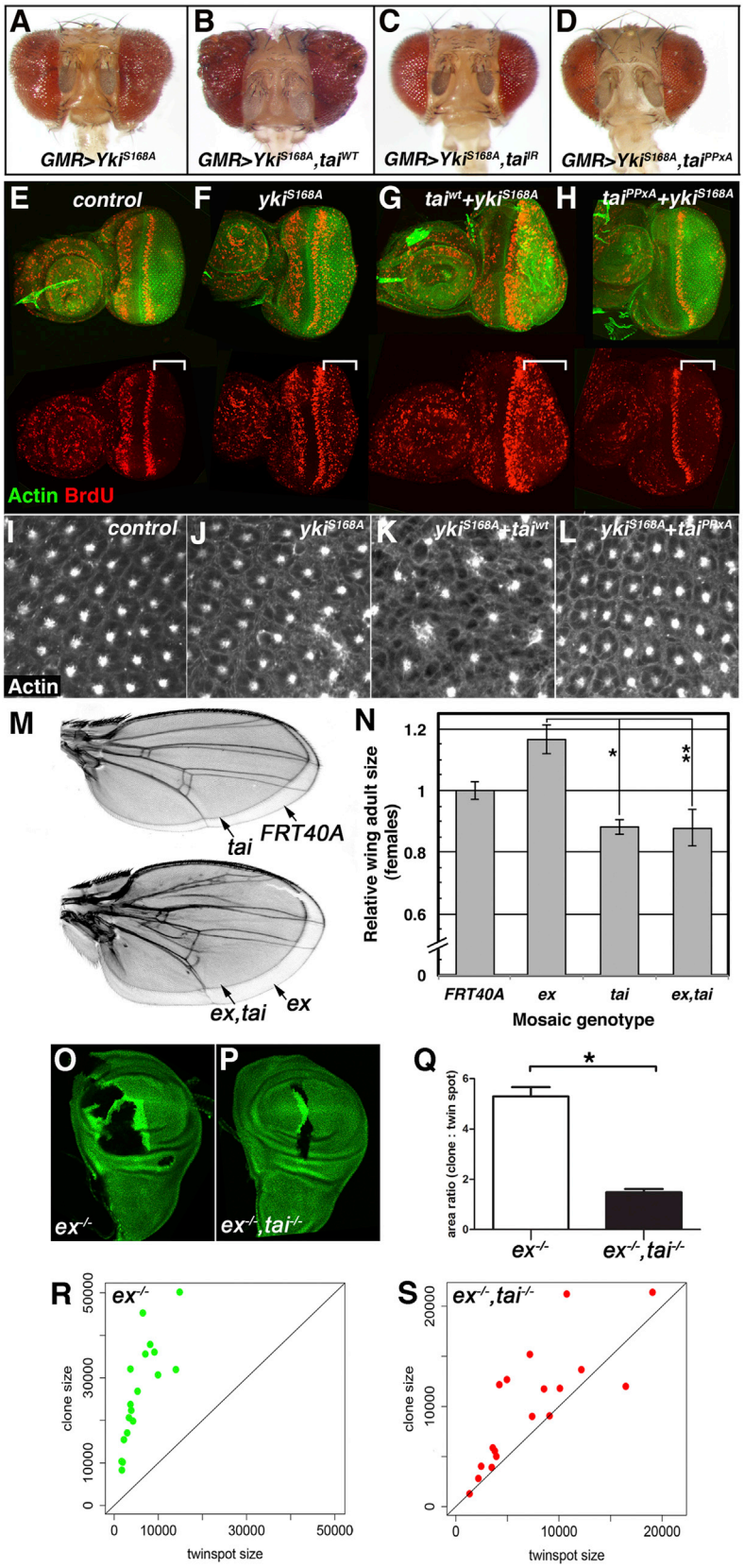

Figure 3. Yki Requires Its Interactor Tai to Drive Tissue Hyperplasia

(A–D) Adult female heads expressing yki^{S168A}, yki^{S168A}+tai^{WT}, yki^{S168A}+tai^{IR}, or yki^{S168A}+$tai^{PPxA1,2}$.

(E–H) Paired top-bottom panels of third instar eye discs of the indicated genotypes stained with FITC-phalloidin (green) to visualize F-actin and anti-BrdU (red) to visualize S phases. Bracket in each lower panel denotes post-mitotic region posterior to the MF. Note the enhancing effect of co-expressed Tai on Yki^{S168A}-driven ectopic S-phase entry behind the MF (F) versus (G) and the opposite suppressive effect of $Tai^{PPxA1,2}$ (F) versus (H).

(I–L) Magnified views of FITC-phalloidin staining posterior to the MF in the same genotypes as in (E)–(H) showing opposing effects of Tai and $Tai^{PPxA1,2}$ on spacing between the F-actin-enriched apical tufts of adjacent Yki^{S168A} photoreceptor clusters.

(M and N) Overlay and quantitation of *Ubx>Flp* adult wings mosaic for a control chromosome (*FRT40A*; n = 6; set as 1.0) versus a *tai* null (tai^{61G1}; n = 11) or an *ex* allele (ex^{e1}; n = 7) versus double mutant for *ex* and *tai* (ex^{e1},tai^{61G1};n = 6). SDs are shown in (N) (*p = 3.0e-5, **p = 1.0e-5).

(O and P) L3 wing discs containing heat shock-FLP induced clones of ex^{e1} (O) or ex^{e1},tai^{61G1} (P) homozygous cells (lacking GFP) and control twinspots (strong GFP signal).

(Q–S) Quantitation of individual ex^{e1} and ex^{e1},tai^{61G1} clone:twinspot size ratios plotted in (R) and (S) relative to a hypothetical linear 1:1 ratio (black line). SEMs are shown in (Q) (n = 18 for both genotypes, *p = 2.36e-11).

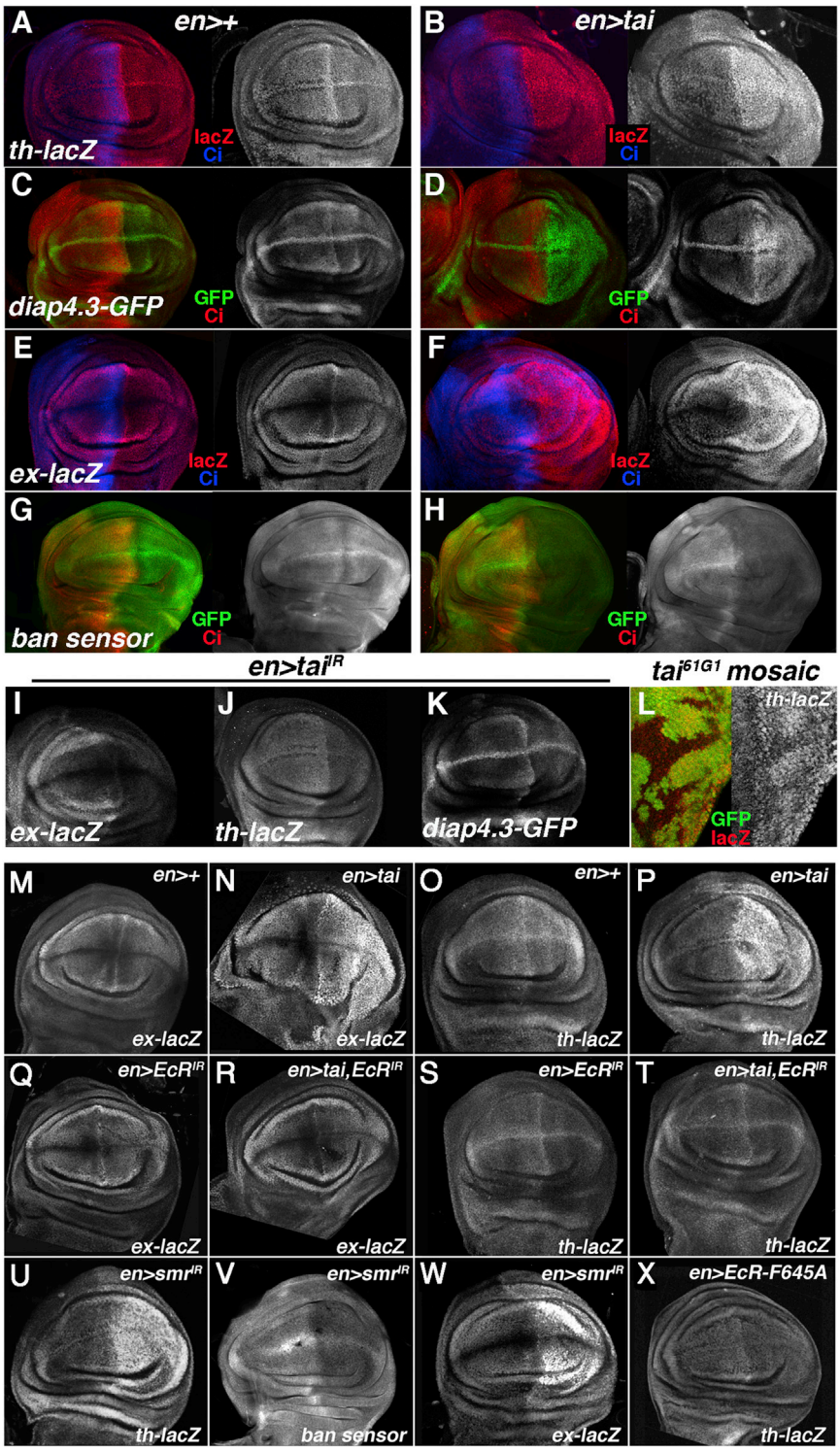

Figure 4. Tai Modulates Expression of Classical Yki-Responsive Genes

(A–H) 3rd instar wing discs stained with anti-Ci and processed to detect β-galactosidase (lacZ) or GFP expression from the Yki activity reporters (A and B) *th-lacZ*, (C and D) *diap4.3-GFP*, (E and F) *ex-lacZ*, and (G and H) *ban sensor-GFP* in the background of *engrailed-Gal4* alone (A, C, E, and G) or in combination with *UAS-tai* (B, D, F, and H).

(I–K) Activity of the indicated Yki-activity reporters in L3 wing disc with depleted Tai in the P-domain (*en>tai^{IR}*).

(L) Anti-β-gal staining (red) to detect *th-lacZ* expression in L3 eye discs carrying clones of *tai^{61G1}* mutant cells marked by the absence of GFP (green).

(M–T) Anti-β-gal (lacZ) staining to detect expression of the *ex-lacZ* or *th-lacZ* enhancer trap lines in L3 wing discs expressing *tai* (N and P), an *EcR.A* RNAi transgene (*EcR^{IR}*) (Q and S), or both transgenes together (*tai,EcR^{IR}*) (R and T).

(U–W) Expression of *th-lacZ*, *ex-lacZ*, and the *ban-sensor* in L3 wing discs with *enGal4*-driven expression of a *smrter* RNAi transgene (*smr^{IR}*) in the P domain.

(X) Anti-β-gal staining to detect *th-lacZ* expression in an L3 wing disc expressing the *EcR.A-F645A* dominant-negative allele from the *enGal4* driver. A:P is left to right in all images.

(Chen et al., 2010; Ling et al., 2010; Robinson et al., 2010). Expression of a version of Crumbs containing only the transmembrane and cytoplasmic domains (Crb^{intra}) in the developing wing induces an adult blistering effect related to its role in apicobasal polarity and a separable enlarged-wing phenotype that is suppressed by heterozygosity for *yki* (Robinson et al., 2010). A *tai* null allele and two *tai* hypomorphs (*tai^{61G1}*, *tai^{k15101}*, and *tai^{01351}*) also dominantly suppress the enlarged size of Crb^{intra} (*en>crb^{intra}*) wings (Figures S4F–S4I). Although *tai* dosage could theoretically also affect Crb^{intra}-induced blistering, the common sensitivity of Crb^{intra}-expressing cells to *yki* and *tai* gene dosage is consistent with Tai interacting with Yki and co-regulating a pro-growth transcriptional program in developing wing and eye tissue.

Tai Requires EcR to Activate *ex* and *thread* Transcription

In view of the physical and functional interactions between Tai and Yki, *tai* alleles were tested for effects on expression of canonical Yki-target genes in imaginal disc cells. Depletion of Tai with *en>tai^{IR}* lowers expression of the *expanded* (*ex-lacZ*), *thread/Diap1* (*th-lacZ* and diap4.3-GFP), and *e2f1* (*e2f1-lacZ*) transcriptional reporters in the P compartment of L3 wing discs (Figures 4I–4K and S5A). A second *tai* RNAi transgene (TRiP *HMS00673*) with a distinct shRNA targeting sequence also reduces expression of the *ex-lacZ* and *th-lacZ* reporters, although more weakly (Figures S5D and S5E). Homozygosity for the *tai^{61G1}* null allele reduces expression of *th-lacZ* and *e2f1-lacZ* in the L3 eye disc posterior to the morphogenetic furrow (MF) (Figures 4L and S5C). Reciprocally,

ex and *th* reporters show elevated expression in the P compartment of *en>tai* wing discs (Figures 4A–4F and S5B). A transgene encoding a version of Tai lacking the N-terminal bHLH domain (Jang et al., 2009) retains the ability to activate *ex-lacZ* in disc cells (Figures S5F and S5G), indicating an interaction with the BTB-domain protein Abrupt is not required for Tai to induce *ex*. These Tai-expressing clones project slightly away from the surface of the epithelium (data not shown), and sections across their base thus appear as "rings" of Yki hyperactivity (e.g., compare the two clones highlighted by arrows in Figure S5G). Tai overexpression also induces activity of the pro-growth miRNA *bantam* (*ban*) as detected by reduced expression of a *GFP-ban* sensor (Figures 4G and 4H), which contains *ban* complementary sites in the 3′UTR of a *GFP* mRNA (Brennecke et al., 2003).

Chromatin immunoprecipitation (ChIP) studies by the modENCODE Project have identified EcR-association peaks within the *D. melanogaster* genome in close proximity to the Yki-induced genes *ex*, *thread*, *ban*, and *e2f1* (modEncode Consortium et al., 2010). Within the *ban* promoter, one of these EcR-association peaks overlaps binding sites for Yki:Mad heterodimers (Oh and Irvine, 2011). ChIP analysis of an inducible, tagged form of Tai detects significant enrichment for this segment of the *ban* promoter (*ban-C12*) (nomenclature according to Oh and Irvine, 2011) in induced cells versus untreated cells (Cu versus NT; Figures S5J and S5K). Control primer sets corresponding to two randomly selected areas of the *ban* promoter (*ban-upstream1*, *ban-upstream2*) show little to no enrichment, as does a *ban* promoter region that interacts with Yki but lacks a coincident EcR-association peak (*banA*) (modEncode Consortium et al., 2010; Oh and Irvine, 2011). Although the degree of Tai association with the *ban-C12* region is relatively moderate, it is nonetheless equivalent to the degree of association of the Tai cofactor with the EcR-binding site in the *Broad* promoter (*EcB* in Figures S5J and S5K) (Bernardo et al., 2014), suggesting similar levels of Tai occupancy on each EcR-interaction site.

Tai influences gene expression via its cognate transcription factor EcR in germline cells and oocyte border cells (Bai et al., 2000; König et al., 2011). To test the requirement for EcR in Tai-driven induction of Yki-responsive genes, an *EcR* RNAi transgene directed at all three EcR isoforms (EcR^{IR}) was used to deplete EcR from wing disc cells. EcR depletion alone had minimal effect on the *ex-lacZ* and *th-lacZ* reporters in L3 wing discs, but eliminated their induction by co-expressed Tai (Figures 4M–4T). RNAi depletion of the EcR-associated transcriptional repressor Smrter (Smr) (Tsai et al., 1999) strongly induces expression of *ex-lacZ*, *th-lacZ*, and suppresses expression of the *GFP-ban* sensor in the larval wing disc (Figures 4U–4W), but has no obvious effect on the unrelated reporter transgene *Serrate-lacZ* (Figures S5H and S5I). The opposing effects of *tai* and *smr* alleles suggest that EcR contributes to both repression and activation of Yki-regulated genes in L3 wing cells. Consistent with this hypothesis, the *EcR.A-F645A* dominant-negative allele, which is deficient in EcR-mediated gene activation but not repression (Cherbas et al., 2003), moderately lowers *th-lacZ* expression among P-domain cells (Figure 4X). These effects of *EcR* and *smr* alleles on Yki-activity reporters are consistent with a role for Tai in modulating Hippo-regulated gene expression in L3 disc cells.

Tai Is Dispensable for Yki Induction of Classic Hippo-Regulated Genes

One explanation for the role of Tai in Yki-driven organ overgrowth is that the Yki:Tai interaction is required for Yki to efficiently stimulate transcription of its established target genes. To test this hypothesis, the effects of *tai* depletion were assayed on transcriptional reporters for the classic Hippo target genes *ex* and *ban*. Although Tai can affect *ex* expression in otherwise WT disc cells (see Figure 4), RNAi depletion of Tai does not prevent transgenic Yki from activating the *ex-lacZ* transcriptional reporter in most of the L3 wing disc, despite suppressing P-domain overgrowth (Figures 5A–5C). Cells along the dorsoventral boundary of the pouch appear to be an exception to this rule, as *ex-lacZ* expression in *en>yki,*tai^{IR} discs is mildly reduced in this region (arrows, Figure 5C). In a reciprocal test, depletion of Yki effectively blocks *ex-lacZ* induction by Tai throughout a majority of the L3 wing disc (Figures 5D–5G), indicating that Yki inputs on *ex* expression are dominant over those from Tai. To test the epistatic relationship between Yki and Tai in control of a *ban* transcriptional reporter, expression of the *ban2.5-lacZ* reporter was analyzed in clones of *ex*, *tai*, or compound mutant *ex,tai* cells in L3 wing discs. Similar to the *ex-lacZ* reporter, Yki-dependent activation of the *ban2.5-lacZ* reporter in *ex* mutant cells is not appreciably suppressed by concurrent loss of *tai* (Figures 5H–5J).

To further test whether suppression of Yki phenotypes by the tai^{IR} and $tai^{PPxA1,2}$ transgenes can be uncoupled from expression of canonical Yki targets, qPCR analysis of the *ex* and *cyclin E* (*cycE*) mRNAs was carried out from RNAs harvested from L3 wing discs expressing either Yki alone, Yki with Tai co-depleted, or Yki with the $Tai^{PPxA1,2}$ dominant-negative allele (Figures 6A and 6B). Removal of Tai did not significantly suppress Yki induction of either of these classic Hippo target mRNAs. Co-expression of $Tai^{PPxA1,2}$ also had no effect on *ex* and *cycE* mRNA induction despite suppressing Yki-driven P-compartment overgrowth. These data indicate that Yki induces the *ex* and *cycE* mRNAs independent of its interaction with Tai.

nanos and *piwi* Are Induced by Hyperactive Yki and Tai in Wing Discs

The uncoupling of a role for Tai in Yki-driven growth from its role in induction of classic Hippo target genes implies that Tai supports an as yet undefined portion of a transcriptional program induced by hyperactive Yki in disc cells. To identify Yki-induced/Tai-dependent genes, RNAs harvested from L3 wing discs expressing either Yki (*en>yki*), or Yki in combination with Tai-depletion (*en>yki+*tai^{IR}) were analyzed by high-throughput sequencing. This analysis generated mapped reads corresponding to more than 12×10^3 transcripts (Figure 6C; Table S1). A subset of these wing disc mRNAs was designated as "candidate Yki-induced mRNAs" based on a greater than 2-fold increase ($\log_2\Delta > 0.8$) in read frequency in experimental (*en>yki*) versus control (*en>*) samples (Table S2); this group includes the established Yki targets *ex* and *kibra* (Genevet et al., 2010; Hamaratoglu et al., 2006). A subset of candidate Yki-induced mRNAs is reduced in abundance ($\log_2\Delta < -0.8$) upon co-depletion of Tai (Table S3). This group includes factors with diverse predicted functions, including a set of RNA regulatory factors expressed in the germline (e.g., *nanos*, *piwi*, *blanks*, *CG17018*, *Argonaute-3*, *sister of Yb*, *qin*, and *krimper*) (Chintapalli et al., 2007), but lacks

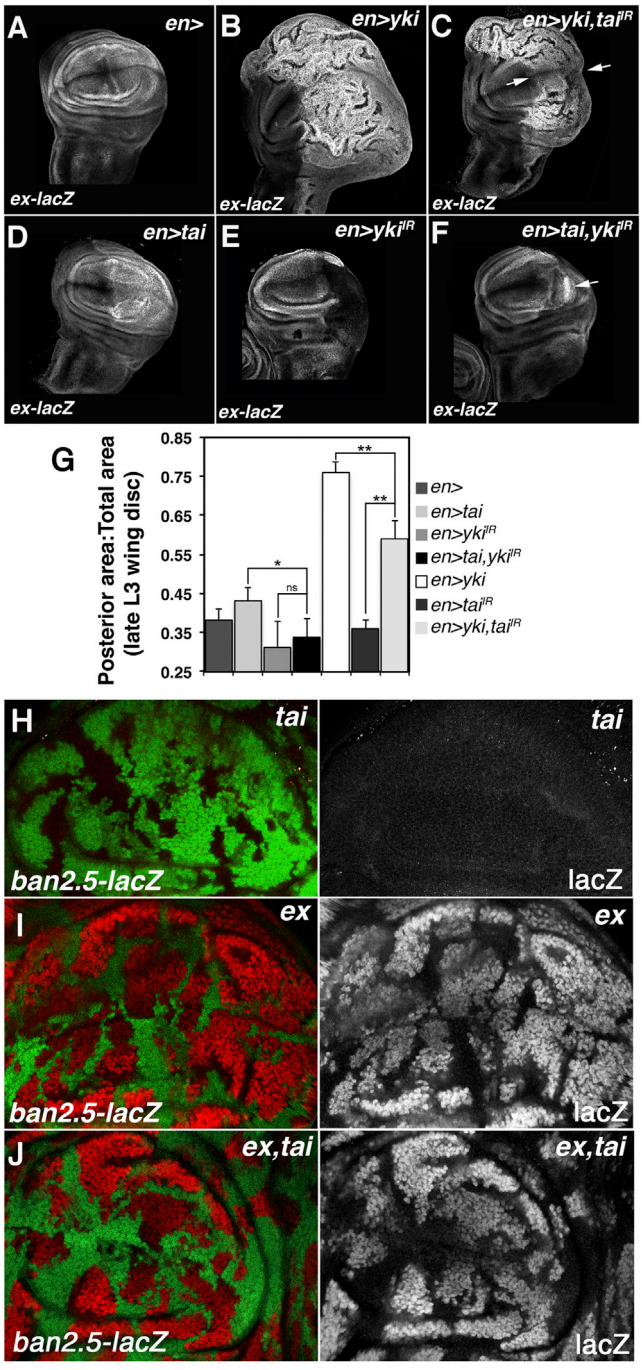

Figure 5. Tai Is Not Required for Induction of *ex* or *ban* by Yki Hyperactivity

(A–F) L3 wing discs stained with anti-β-gal to detect expression of the *ex-lacZ* enhancer trap in the indicated genetic backgrounds. Arrows in (C) denote reduced *ex-lacZ* expression along the dorsal-ventral boundary.

(G) Corresponding quantitative analysis of the posterior compartment ratio (P area/total area) among L3 wing discs in (A)–(F) (SDs are shown; n = 10 for *en>+* and *en>tai*, n = 4 for *en>yki^{IR}*, n = 11 for *en>tai,yki^{IR}*, n = 9 for *en>yki*, n = 12 for *en>tai^{IR}*, n = 8 for *en>yki,tai^{IR}*– *, **see *Statistics* in Supplemental Experimental Procedures; ns = not significant).

(H–J) Anti-β-gal staining (red) to detect *ban2.5-lacZ* expression in *tai^{61G1}* mutant (H), *ex^{e1}* mutant (I), or *tai^{61G1},ex^{e1}* double-mutant (J) clones in the L3 wing pouch marked by the absence of GFP (green).

ex and *kibra*, consistent with a lack of a requirement for Tai induction of classic Hippo-responsive genes.

Direct analysis of select candidate Yki-induced mRNAs by qPCR confirmed that depletion of Tai in Yki-overexpressing L3 wing disc cells blocks induction of the RNA regulatory factors *nanos* and *piwi*, the Ec-induced gene *Eig71Ee*, and the secreted insulin-like peptide *dILP-8* (Figure 6D). A second, weaker *tai^{IR}* transgene (*HMS00673*) also partially suppressed Yki-induction of *nanos*, *dILP-8*, and *Eig71Ee* but did not alter induction of *piwi*, perhaps indicative of a lower threshold of Tai required for Yki to activate *piwi* transcription (Figure S6A). Importantly, co-expression of Tai enhances Yki-driven induction of the *nanos* and *piwi* mRNAs, while Tai^{PPxA1,2} blocks induction of *nanos* and *dILP-8* and shows reduced ability to enhance *piwi* expression. Tai thus requires its PPxY motifs, which can bind to Yki, to support Yki-driven induction of these mRNAs. RNAi depletion also supports a selective role for EcR isoforms in the Tai-dependent segment of the Yki-induced transcriptome in L3 wing disc cells (Figure S6B). Transgenes targeting all three EcR isoforms (*EcR^{IR}*), the EcR.A isoform (*EcR.A^{IR}*), or the EcR.B1 isoform (*EcR.B1^{IR}*) do not affect Yki-induction of the *ex* or *cycE* mRNAs, but can individually suppress induction of *nanos* and *piwi*. Induction of *dILP-8* was effectively inhibited only by pan depletion of EcR, whereas individual depletion of EcR.A or EcR.B1 inhibited induction of *Eig71Ee*, suggesting that the remaining EcR isoform, EcR.B2, may contribute to activation of *dILP-8* and repression of *Eig71Ee*. In sum, the lack of an effect of *tai^{PPxA1,2}* or *tai^{IR}* on Yki-induction of the classic Hippo targets *ex* and *cycE* (Figure 6B versus Figure 6D) contrasts with the requirements for Tai, and apparently EcR as well, in Yki-mediated control of the *nanos*, *piwi*, *dILP-8*, and *Eig71Ee* mRNAs in L3 wing disc cells.

The *nanos*, *piwi*, and *dILP-8* mRNAs all share a pattern of highly enriched expression in the germline (Chintapalli et al., 2007). The *nanos* and *piwi* gene products act cell autonomously to support self-renewing divisions of GSCs (Cox et al., 1998; Forbes and Lehmann, 1998; Kobayashi et al., 1996; Lin and Spradling, 1997), and in the case of *piwi*, ectopic expression is sufficient to increase somatic cell division (Cox et al., 2000). *nanos* and *piwi* expression were analyzed in L3 wing discs using an anti-Nanos antibody (Asaoka-Taguchi et al., 1999) and a *lacZ* enhancer trap inserted into the *piwi* locus (*piwi^{1}* or *piwi-lacZ*) (Lin and Spradling, 1997). Nanos protein is expressed at very low levels in lysates of control discs but induced in Yki-expressing discs in a Tai-dependent manner similar to its mRNA (Figure 7A). Expression of *piwi-lacZ* is also induced in P-domain wing disc cells that express the *yki* transgene (Figures 7B–7E). This induction of *piwi-lacZ* by transgenic Yki is blocked in cells also depleted of Tai (Figure S6C), and this correlates with a reduced degree of tissue expansion and folding in the areas of the dorsal and ventral wing hinge. Significantly, activating endogenous Yki by RNAi depletion of the Wts kinase (*wts^{KK101055}*) leads to mild disc growth, consistent with a partial loss of Wts, and also elevates *piwi-lacZ* expression (Figure 7F). Induction of *piwi-lacZ* by Yki expression or Wts loss is most robust in the dorsal and ventral regions of the wing hinge, suggesting that cells in these areas activate a GSC-like program most strongly. Individual depletion of Nanos or Piwi, with either a *nanos^{IR}* line (*IR-1*) that efficiently reduces Nanos protein levels in *en>yki* discs (Figure S7A) or two *piwi^{IR}* lines (IR-1 and IR-2), suppresses the

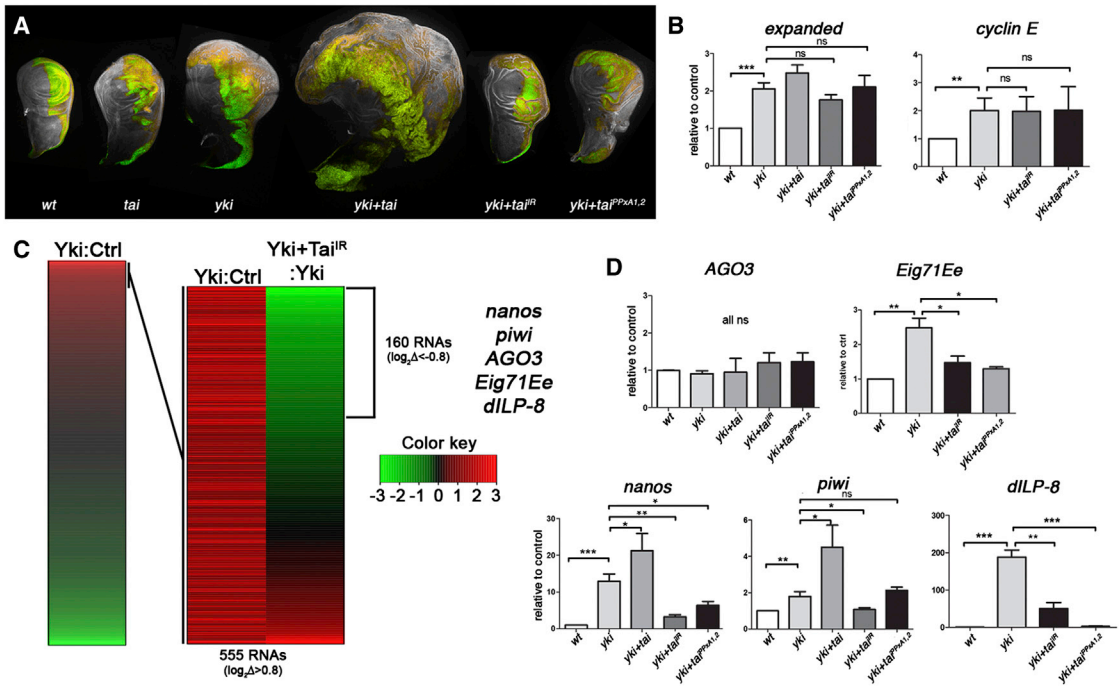

Figure 6. Identification of Yki-Induced, Tai-Dependent RNAs in Larval Wing Discs

(A) Late L3 *enGal4,UAS-GFP* wing discs from control (*wt*) animals or those expressing the indicated transgenes stained with phalloidin-AlexaFluor-594 (gray) to visualize F-actin (images to scale).

(B) Quantitative real-time PCR (qPCR) analysis of *expanded* and *cyclin E* mRNA levels in late L3 wing discs carrying the indicated transgenes in combination with *enGal4*.

(C) Color-coded heat map illustrating changes in abundance of individual RNAs between control versus Yki-expressing (Yki:Ctrl), and Yki-expressing versus Yki-expressing/Tai-depleted (Yki:Yki+Tai^{IR}) late L3 wing discs (see Tables S1, S2, and S3). The Yki:Ctrl heatmap contains 9,303 RNAs, of which 555 are induced >0.8($\log_2$)-fold. Of these, 160 RNAs (bracketed) are suppressed by >0.8($\log_2$) upon Tai depletion.

(D) qPCR analysis of *AGO3*, *Eig71Ee*, *nanos*, *piwi*, and *dILP-8* mRNAs in wing discs of the indicated transgenes in combination with *enGal4*. For all qPCR data, SEMs are shown (n = 3; *p values see *Statistics* in Supplemental Experimental Procedures; ns = not significant).

growth of *en>yki* L3 wing discs and *GMR-yki*^{S168A} transgenic adult eyes with little effect on corresponding WT organs (Figures 7G–7I; see also Figure S6C). Moreover, combining a *nanos*^{I7} hypomorphic allele and a deficiency covering the *nanos* locus (*Df(3L)Exel6183*) also partially suppresses *en>yki* L3 wing disc overgrowth (Figure S7B). These requirements for Nanos and Piwi for Yki-driven growth supports a model in which these GSC factors are ectopically induced by a hyperactive Yki-Tai complex as one element of a transcriptional program that is normally repressed by the Hippo pathway in developing somatic epithelia.

DISCUSSION

Studies of the *Drosophila* Hippo pathway have uncovered an array of cytoplasmic regulators and nuclear factors that modulate expression of a fairly small set of transcriptional targets. Yet the association of the Hippo nuclear effector Yki with a large number of sites in the fly genome (Oh et al., 2014) implies links to a wider array of targets and cellular processes. Here we show that the EcR-coactivator protein Tai plays a dual role as a regulator of Yki-induced genes during normal development and a key mediator of the effect of hyperactive Yki on cells with disrupted Hippo signaling (model, Figure 7J). Tai supports normal developmental growth by controlling expression of classic Yki targets *ex*, *thread*, *bantam*, and *e2f1*, but its role on these genes is largely subordinate to inputs from Yki. EcR is required by Tai to induce *ex* and *thread* and the EcR-bound repressor Smrter is also required to repress *ex*, *thread*, and *ban*, suggesting that Tai and other EcR components provide parallel, but subordinate, inputs to Yki on these developmentally regulated genes. Tai can interact with Yki via PPxY motifs present in the Tai TAD, and this interaction links hyperactive Yki to a previously undefined segment of the Yki-induced transcriptome that includes the GSC factors *nanos* and *piwi*. The ability of the Tai^{PPxA1,2} protein to mildly retard the growth of otherwise WT tissues (e.g., Figure S2B versus Figure S2F) suggests that a Tai-Yki complex plays a small role in normal developmental growth, perhaps during developmental stages other than those examined here. Critically, under conditions of Yki hyperactivity, the Yki-Tai interaction becomes central to induction of an additional set of transcriptional targets in L3 discs, including *nanos* and *piwi*, which support tissue overgrowth. These findings reveal that Tai plays a key role in determining the transcriptional output of hyperactive Yki and significantly expand knowledge of Yki-induced genes by highlighting a division within the Yki-induced transcriptome into Tai-dependent and -independent target genes.

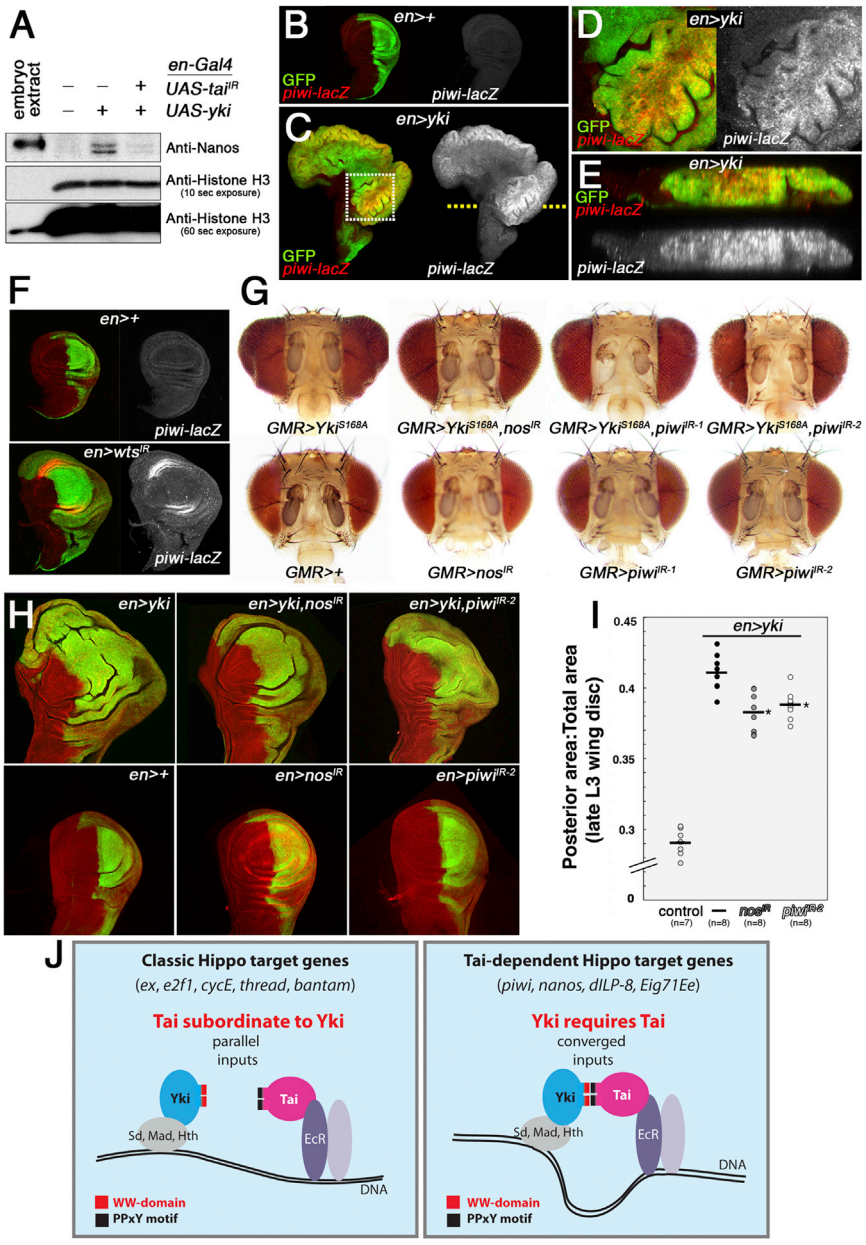

Figure 7. Nanos and Piwi Are Induced by Yki and Are Required for Disc Hyperplasia

(A) Western blot of Nanos protein (top) in L3 wing discs of the indicated genotypes. Embryo extract (far left) is enriched for Nanos. Anti-histone H3 (H3) is included as a loading control (middle). A longer exposure detects histone H3 in embryonic extract (lower).

(B–E) *piwi-lacZ* expression (red) in control *en>GFP* (B) or *en>yki,GFP* (C–E) late L3 wing discs. (D) and (E) are magnified views of areas boxed in (C) or cross-sectional view through the dotted line in (C).

(F) Expression of the *piwi-lacZ* reporter in control (top) and *en>warts*^{IR} (bottom) L3 wing discs.

(G) Adult female heads expressing Yki^{S168A} from the *GMR-Gal4* driver alone or in combination with Nanos (*nos*^{IR}) or Piwi (*piwi*$^{IR-1}$ or *piwi*$^{IR-2}$) knockdown.

(H) Late L3 wing discs of the indicated genotypes stained with phalloidin-AlexaFluor-594 to visualize F-actin.

(I) Scatterplot analysis of posterior compartment ratio (P area:total area) among control (*en*>GFP), Yki-expressing (*en>yki*), or in Yki combination with *nos*^{IR} or *piwi*$^{IR-2}$ late L3 wing discs. Black bar is the average ratio for each genotype (*0.01 < p < 0.05 relative to *en>yki* alone).

(J) A proposed model depicting dual roles of Tai in Yki-driven growth programs. Tai supports expression of classic Yki targets during normal disc development, but is subordinate to Yki (left). In cells with elevated Yki activity, the Tai:Yki interaction is required to induce a distinct transcriptional program including the GSC factors Nanos and Piwi (right).

Induction of the normally germline-specific *nanos* and *piwi* RNAs in imaginal disc cells by hyperactive Yki implies that inactivation of the Hippo pathway engages a transcriptional program that diverges from normal development. In addition to *nanos* and *piwi*, a significant fraction of the candidate Yki-induced/Tai-dependent genes (Table S3) display germline-enriched patterns of expression (Chintapalli et al., 2007). The *dILP-8* mRNA falls into this category as well; it is normally expressed mainly in the adult ovary, but is ectopically induced by Yki in a Tai-dependent manner in wing discs (this study) and by mutations that produce neoplastic wing disc tumors (Colombani et al., 2012; Garelli et al., 2012), suggestive of common mechanisms linking expression of germline genes to abnormal disc growth. However, unlike the secreted factor dILP-8, Nanos and Piwi proteins act autonomously in cells that express them. Nanos complexes with other RNA binding proteins such as Pumilio to block translation of germline mRNAs encoding differentiation factors (Asaoka-Taguchi et al., 1999; Forbes and Lehmann, 1998) and supports survival of germ cells by repressing translation of the pro-apoptotic factor Hid (Sato et al., 2007). Intriguingly, the miR *bantam* is required to maintain female GSCs (Yang et al., 2009) and directly represses the *hid* mRNA (Brennecke et al., 2003), suggesting that Nanos and *bantam* may co-regulate the *hid* mRNA downstream of hyperactive Yki. Piwi interacts with piRNAs in the germ cell cytoplasm to repress target mRNAs but also has a critical nuclear role in formation of repressive chromatin on specific genomic loci (Klenov et al., 2014; Le Thomas et al., 2013). Both Nanos and Piwi play key roles in blocking differentiation and supporting self-renewing divisions in the germline (Cox et al., 1998, 2000; Forbes and Lehmann, 1998; Kobayashi et al., 1996; Lin and Spradling, 1997), suggesting that disc cells with hyperactive Yki autonomously adopt elements of a germline transcriptional program. As depletion of either factor in disc cells blunts Yki-driven growth but has no effect on control tissues, Nanos and Piwi behave as required elements of a larger transcriptional program that is engaged by hyperactive Yki in disc cells. The physiologic correlate to this GSC-like growth program

is unclear, although a similar program is engaged in larval brain cells lacking the insulator accessory protein l(3)Mbt (Janic et al., 2010) and may be associated with Yki-mediated regeneration of damaged epithelia (Grusche et al., 2011; Sun and Irvine, 2011). Piwi-related proteins are expressed in somatic stems cells of the planarian flatworm *S. mediterranea* and are required for these cells to drive regenerative growth (Reddien et al., 2005), further supporting a link between Yki and Piwi in regenerative tissue growth. The ectopic expression of *piwi* and *nanos* homologs in human cancer cells and their roles in supporting cancer cell proliferation (reviewed in Bonnomet et al., 2008; Ross et al., 2014; Strumane et al., 2006) imply that GSC factors can also support aberrant tissue growth in vertebrates, perhaps by promoting self-renewing divisions of cancer stem cells as proposed for the vertebrate Yki homolog Yap1 (reviewed in Mo et al., 2014).

In addition to effects on disc growth, co-overexpression of Yki and Tai appears to enhance levels of F-actin in L3 wing discs, as detected by phalloidin staining (e.g., Figure 6A), suggesting that Yki and Tai modulate expression of factors involved in actin cytoskeleton dynamics. Given that F-actin can modulate Yki activity (Fernández et al., 2011; Sansores-Garcia et al., 2011), this phenomenon could further augment the effect of Yki and Tai on the Hippo transcriptome. Alternatively, effects of Yki and Tai on the actin cytoskeleton could occur via a shared downstream target that stimulates F-actin polymerization during motility or cell-shape changes associated with tissue remodeling, as occurs during pupal morphogenesis.

The physical interaction between the Yki and Tai proteins, and the genetic requirements for EcR and Smrter in control of Hippo target genes, suggests that the Ec and Hippo pathways could share additional nuclear components and/or transcriptional targets. Consistent with this hypothesis, hyperactive Yki can promote transcription by recruiting a histone methyltransferase complex containing the NCOA-6 and Trithorax-related (Trr) proteins (Oh et al., 2014), which are also part of an EcR-associated transcriptional complex (Carbonell et al., 2013; Mohan et al., 2011; Sedkov et al., 2003). In addition, the *Eig71Ee* mRNA responds to the 20E pulse at the L3-pupal transition (Graveley et al., 2011) and, as shown here, behaves as a Yki-inducible/Tai-dependent transcript in L3 larval wings, implying some degree of reciprocal crosstalk between the pathways. It is also notable that Tai and Yki are involved in common cell biological processes, but have not as yet been shown to perform these roles via interaction with each other. Yki acts in enteroblasts to support regenerative division of intestinal stem cells (reviewed in Lucchetta and Ohlstein, 2012), while Tai supports stem cell development in the female germline (König et al., 2011). Intriguingly, the hormone estrogen and the Tai-ortholog NCOA3, which interacts with the estrogen receptor, each support stem cell pools in vertebrates (Chitilian et al., 2014; Nakada et al., 2014), indicative of a potential conserved link between hormone signaling and stem cell renewal. Tai and Yki also each act cell autonomously to support invasive behavior of somatic border cell clusters in the ovary (Bai et al., 2000; Lucas et al., 2013). Thus, one goal of further studies will be to probe more deeply into the developmental and homeostatic contexts in which the Ec and Hippo pathways converge on the Tai-Yki complex and to identify relevant and shared transcriptional targets in each biological setting.

EXPERIMENTAL PROCEDURES

Genetics

All crosses were maintained at 25°C unless otherwise noted. For RNA analyses, 24-hr embryos and L1 larvae were shifted to 28°C, and discs were collected from late L3 wandering-stage larvae. Alleles used in these studies (Bloomington stock number indicated) are as follows: *Df(2L)ED678* (#8906), tai^{05809} (#12172), tai^{15101} (#10453), $nanos^{17}$ (#3285), *Df(3R)Exel6183* (#7662), *UAS-tai* (#6378), *UAS-taiΔB* (#28273), *UAS-tai-IR-1/2* (#28971, #32885), *FRT40A*,tai^{61G1}*-FRT40A* (#6379), ex^{e1}*-FRT40A* (#44249), tai^{61G1}, ex^{e1}*-FRT40A, UAS-*yki^{S168A}*:V5* (#28818), *UAS-EcR.A-F645A* (#9452), *UAS-EcR-IR* (pan-EcR, #29374), *UAS-EcR.A-IR* (#9452), *UAS-EcR.B1-IR* (#9329), *UAS-smrter-IR* (27068), th^{lc58} (*th-lacZ*; #12093), $piwi^{1}$ (#43637), *UAS-nanos-IR* (#28300), *UAS-piwi-IR-1/2* (#34866, #33724), ex^{697} (*ex-lacZ,* #44248), $e2f1^{rM729}$ (*e2f1-lacZ*, #34054), *da-Gal4* (#55851), and *MS1096-Gal4* (#8860) obtained from the Bloomington *Drosophila* Stock Center. *UAS-yki-IR* (v104523) and *UAS-warts-IR* (v106174) were obtained from the Vienna Drosophila Resource Center (VDRC). Other alleles used were *enGal4/CyO*, *ey-FLP;ubi-GFP-FRT40A*, *Ubx-Flp;ubiGFP-FRT40A*, *UAS-yki-GFP*, *Serrate-lacZ* (R. Read), *ban2.5-lacZ*, (K. Irvine), *UAS-sd-IR* and *DIAP4.3-GFP* (J. Jiang), *ban-sensor GFP* (G. Halder), *GMR-Gal4,UAS-*yki^{S168A}*:GFP* (K. Harvey), *UAS-yki* (D.J. Pan), and *hsFLP;Act>CD2>Gal4* (J. Treisman). The *UAS-*$tai^{PPxA1,2}$ transgene was generated by standard approaches; transgenic services were provided by BestGene.

Immunofluorescence Microscopy

Immunostaining and confocal microscopy performed using standard procedures. Primary antibodies include mouse anti-β-Gal 1:1000 (Promega); rabbit anti-Tai (1:1000; D. Montell); mouse anti-Ci (1:50) and mouse anti-BrC-Z3 (1:100) (DSHB); rabbit anti-Nanos (1:1000; A. Nakamura), anti-histone H3 (1:10,000; Abcam); BrdU assays performed as described previously (Robinson et al., 2010) with mouse anti-BrdU (1:100; Becton Dickinson). Secondary antibodies are goat anti-mouse-Cy3 and goat anti-mouse-Cy5 (1:100; Jackson Labs). Phalloidin-AlexaFluor-594 and 488 (1:100; Life Technologies) were used to detect F-actin.

Immunoprecipitation and ChIP in Cultured Cells

Drosophila S2 cell culture, transfection, and immunoprecipitation analysis were performed as described in Gilbert et al. (2011). *tai* expression constructs were generated from a *tai* ORF plasmid (gift of D. Montell) into the streptavidin binding peptide (SBP), $CuSO_4$-inducible *pMK33* vector (Kyriakakis et al., 2008). *tai-pMK33* variants generated via site-directed mutagenesis. WT and WW mutant versions of HA-tagged Yki are described previously in Gilbert et al. (2011). For ChIP, an S2 clone stably transformed by *pMK33-SBP-tai* was induced with 0.5 mM $CuSO_4$, cross-linked in 1% formaldehyde, and quenched in 125 mM glycine. Lysates prepared in ice-cold nuclei lysis buffer (5 mM PIPES [pH 8.0], 85 mM KCl, 0.5% NP-40) plus protease inhibitors (Roche), followed by equal volume of SDS lysis buffer (1% SDS, 10 mM EDTA, 50 mM Tris-HCl [pH 8.0]) plus protease inhibitors (Roche), and then sonicated prior to centrifugation. Streptavidin-agarose beads (Thermo Scientific) were mixed with lysates and then sequentially washed (0.1% SDS, 1% Triton X-100, 2 mM EDTA, 20 mM Tris-HCl [pH 8.0], 150 mM NaCl, then 0.1% SDS, 1% Triton X-100, 2 mM EDTA, 20 mM Tris-HCl [pH 8.0], 500 mM NaCl, then 0.25 M LiCl, 1% NP 40, 1% sodium deoxycholate, 1 mM EDTA, 10 mM Tris-HCl [pH 8.0]; 2× with TE) and eluted (50 mM Tris/HCl [pH 7.4], 250 mM NaCl 0.5% NP-40, 0.1% sodium deoxycholate, 4 mM biotin), extracted, and suspended in TE buffer.

SUPPLEMENTAL INFORMATION

Supplemental Information includes Supplemental Experimental Procedures, seven figures, and three tables and can be found with this article online at http://dx.doi.org/10.1016/j.devcel.2015.05.010.

AUTHOR CONTRIBUTIONS

C.Z. and B.S.R. conceived and carried out experiments, analyzed data, and contributed to writing the paper. H.Z., L.Z., and W.X. designed and carried

out protein:protein interaction assays. P.K.B. contributed data for revision. P.J. and B.Y. carried out and analyzed RNA-seq experiments. A.V. and K.H.M. conceived experiments, analyzed data, and wrote the paper.

ACKNOWLEDGMENTS

We apologize for works not cited due to space constraints. We thank D. Montell, K. Harvey, D.J. Pan, J. Jiang, G. Halder, Developmental Studies Hybridoma Bank (DSHB), Bloomington Drosophila Stock Center (BDSC), Transgenic RNAi Project (TRiP), and VDRC for reagents and fly stocks. We also thank members of the K.H.M. and A.V. laboratories for helpful discussion. The work was funded by NIH grants GM105813 to A.V. and K.H.M. and CA123368 to K.H.M.

Received: December 28, 2014
Revised: April 25, 2015
Accepted: May 14, 2015
Published: July 2, 2015

REFERENCES

Asaoka-Taguchi, M., Yamada, M., Nakamura, A., Hanyu, K., and Kobayashi, S. (1999). Maternal Pumilio acts together with Nanos in germline development in Drosophila embryos. Nat. Cell Biol. *1*, 431–437.

Badouel, C., Gardano, L., Amin, N., Garg, A., Rosenfeld, R., Le Bihan, T., and McNeill, H. (2009). The FERM-domain protein Expanded regulates Hippo pathway activity via direct interactions with the transcriptional activator Yorkie. Dev. Cell *16*, 411–420.

Bai, J., Uehara, Y., and Montell, D.J. (2000). Regulation of invasive cell behavior by taiman, a Drosophila protein related to AIB1, a steroid receptor coactivator amplified in breast cancer. Cell *103*, 1047–1058.

Bayer, C.A., Holley, B., and Fristrom, J.W. (1996). A switch in broad-complex zinc-finger isoform expression is regulated posttranscriptionally during the metamorphosis of Drosophila imaginal discs. Dev. Biol. *177*, 1–14.

Bernardo, T.J., Dubrovskaya, V.A., Xie, X., and Dubrovsky, E.B. (2014). A view through a chromatin loop: insights into the ecdysone activation of early genes in Drosophila. Nucleic Acids Res. *42*, 10409–10424.

Bonnomet, A., Polette, M., Strumane, K., Gilles, C., Dalstein, V., Kileztky, C., Berx, G., van Roy, F., Birembaut, P., and Nawrocki-Raby, B. (2008). The E-cadherin-repressed hNanos1 gene induces tumor cell invasion by upregulating MT1-MMP expression. Oncogene *27*, 3692–3699.

Boulan, L., Martín, D., and Milán, M. (2013). bantam miRNA promotes systemic growth by connecting insulin signaling and ecdysone production. Curr. Biol. *23*, 473–478.

Brennan, C.A., Ashburner, M., and Moses, K. (1998). Ecdysone pathway is required for furrow progression in the developing Drosophila eye. Development *125*, 2653–2664.

Brennecke, J., Hipfner, D.R., Stark, A., Russell, R.B., and Cohen, S.M. (2003). bantam encodes a developmentally regulated microRNA that controls cell proliferation and regulates the proapoptotic gene hid in Drosophila. Cell *113*, 25–36.

Carbonell, A., Mazo, A., Serras, F., and Corominas, M. (2013). Ash2 acts as an ecdysone receptor coactivator by stabilizing the histone methyltransferase Trr. Mol. Biol. Cell *24*, 361–372.

Chen, C.L., Gajewski, K.M., Hamaratoglu, F., Bossuyt, W., Sansores-Garcia, L., Tao, C., and Halder, G. (2010). The apical-basal cell polarity determinant Crumbs regulates Hippo signaling in Drosophila. Proc. Natl. Acad. Sci. USA *107*, 15810–15815.

Cherbas, L., Hu, X., Zhimulev, I., Belyaeva, E., and Cherbas, P. (2003). EcR isoforms in Drosophila: testing tissue-specific requirements by targeted blockade and rescue. Development *130*, 271–284.

Chintapalli, V.R., Wang, J., and Dow, J.A. (2007). Using FlyAtlas to identify better Drosophila melanogaster models of human disease. Nat. Genet. *39*, 715–720.

Chitilian, J.M., Thillainadesan, G., Manias, J.L., Chang, W.Y., Walker, E., Isovic, M., Stanford, W.L., and Torchia, J. (2014). Critical components of the pluripotency network are targets for the p300/CBP interacting protein (p/CIP) in embryonic stem cells. Stem Cells *32*, 204–215.

Choi, H., Larsen, B., Lin, Z.Y., Breitkreutz, A., Mellacheruvu, D., Fermin, D., Qin, Z.S., Tyers, M., Gingras, A.C., and Nesvizhskii, A.I. (2011). SAINT: probabilistic scoring of affinity purification-mass spectrometry data. Nat. Methods *8*, 70–73.

Colombani, J., Andersen, D.S., and Léopold, P. (2012). Secreted peptide Dilp8 coordinates Drosophila tissue growth with developmental timing. Science *336*, 582–585.

Cox, D.N., Chao, A., Baker, J., Chang, L., Qiao, D., and Lin, H. (1998). A novel class of evolutionarily conserved genes defined by piwi are essential for stem cell self-renewal. Genes Dev. *12*, 3715–3727.

Cox, D.N., Chao, A., and Lin, H. (2000). piwi encodes a nucleoplasmic factor whose activity modulates the number and division rate of germline stem cells. Development *127*, 503–514.

Delanoue, R., Slaidina, M., and Léopold, P. (2010). The steroid hormone ecdysone controls systemic growth by repressing dMyc function in Drosophila fat cells. Dev. Cell *18*, 1012–1021.

DiBello, P.R., Withers, D.A., Bayer, C.A., Fristrom, J.W., and Guild, G.M. (1991). The Drosophila Broad-Complex encodes a family of related proteins containing zinc fingers. Genetics *129*, 385–397.

Fernández, B.G., Gaspar, P., Brás-Pereira, C., Jezowska, B., Rebelo, S.R., and Janody, F. (2011). Actin-Capping Protein and the Hippo pathway regulate F-actin and tissue growth in Drosophila. Development *138*, 2337–2346.

Forbes, A., and Lehmann, R. (1998). Nanos and Pumilio have critical roles in the development and function of Drosophila germline stem cells. Development *125*, 679–690.

Fristrom, J.W. (1970). The developmental biology of Drosophila. Annu. Rev. Genet. *4*, 325–346.

Garelli, A., Gontijo, A.M., Miguela, V., Caparros, E., and Dominguez, M. (2012). Imaginal discs secrete insulin-like peptide 8 to mediate plasticity of growth and maturation. Science *336*, 579–582.

Gaziova, I., Bonnette, P.C., Henrich, V.C., and Jindra, M. (2004). Cell-autonomous roles of the ecdysoneless gene in Drosophila development and oogenesis. Development *131*, 2715–2725.

Genevet, A., Wehr, M.C., Brain, R., Thompson, B.J., and Tapon, N. (2010). Kibra is a regulator of the Salvador/Warts/Hippo signaling network. Dev. Cell *18*, 300–308.

Ghbeish, N., and McKeown, M. (2002). Analyzing the repressive function of ultraspiracle, the Drosophila RXR, in Drosophila eye development. Mech. Dev. *111*, 89–98.

Ghbeish, N., Tsai, C.C., Schubiger, M., Zhou, J.Y., Evans, R.M., and McKeown, M. (2001). The dual role of ultraspiracle, the Drosophila retinoid X receptor, in the ecdysone response. Proc. Natl. Acad. Sci. USA *98*, 3867–3872.

Gilbert, M.M., Tipping, M., Veraksa, A., and Moberg, K.H. (2011). A screen for conditional growth suppressor genes identifies the Drosophila homolog of HD-PTP as a regulator of the oncoprotein Yorkie. Dev. Cell *20*, 700–712.

Graveley, B.R., Brooks, A.N., Carlson, J.W., Duff, M.O., Landolin, J.M., Yang, L., Artieri, C.G., van Baren, M.J., Boley, N., Booth, B.W., et al. (2011). The developmental transcriptome of Drosophila melanogaster. Nature *471*, 473–479.

Grusche, F.A., Degoutin, J.L., Richardson, H.E., and Harvey, K.F. (2011). The Salvador/Warts/Hippo pathway controls regenerative tissue growth in Drosophila melanogaster. Dev. Biol. *350*, 255–266.

Hamaratoglu, F., Willecke, M., Kango-Singh, M., Nolo, R., Hyun, E., Tao, C., Jafar-Nejad, H., and Halder, G. (2006). The tumour-suppressor genes NF2/Merlin and Expanded act through Hippo signalling to regulate cell proliferation and apoptosis. Nat. Cell Biol. *8*, 27–36.

Hay, B.A., Maile, R., and Rubin, G.M. (1997). P element insertion-dependent gene activation in the Drosophila eye. Proc. Natl. Acad. Sci. USA *94*, 5195–5200.

Henrich, V.C., Tucker, R.L., Maroni, G., and Gilbert, L.I. (1987). The ecdysoneless (ecd1ts) mutation disrupts ecdysteroid synthesis autonomously in the ring gland of Drosophila melanogaster. Dev. Biol. *120*, 50–55.

Hu, X., Cherbas, L., and Cherbas, P. (2003). Transcription activation by the ecdysone receptor (EcR/USP): identification of activation functions. Mol. Endocrinol. *17*, 716–731.

Jang, A.C., Chang, Y.C., Bai, J., and Montell, D. (2009). Border-cell migration requires integration of spatial and temporal signals by the BTB protein Abrupt. Nat. Cell Biol. *11*, 569–579.

Janic, A., Mendizabal, L., Llamazares, S., Rossell, D., and Gonzalez, C. (2010). Ectopic expression of germline genes drives malignant brain tumor growth in Drosophila. Science *330*, 1824–1827.

Klenov, M.S., Lavrov, S.A., Korbut, A.P., Stolyarenko, A.D., Yakushev, E.Y., Reuter, M., Pillai, R.S., and Gvozdev, V.A. (2014). Impact of nuclear Piwi elimination on chromatin state in Drosophila melanogaster ovaries. Nucleic Acids Res. *42*, 6208–6218.

Kobayashi, S., Yamada, M., Asaoka, M., and Kitamura, T. (1996). Essential role of the posterior morphogen nanos for germline development in Drosophila. Nature *380*, 708–711.

Koelle, M.R., Talbot, W.S., Segraves, W.A., Bender, M.T., Cherbas, P., and Hogness, D.S. (1991). The Drosophila EcR gene encodes an ecdysone receptor, a new member of the steroid receptor superfamily. Cell *67*, 59–77.

König, A., Yatsenko, A.S., Weiss, M., and Shcherbata, H.R. (2011). Ecdysteroids affect Drosophila ovarian stem cell niche formation and early germline differentiation. EMBO J. *30*, 1549–1562.

Kwon, Y., Vinayagam, A., Sun, X., Dephoure, N., Gygi, S.P., Hong, P., and Perrimon, N. (2013). The Hippo signaling pathway interactome. Science *342*, 737–740.

Kyriakakis, P., Tipping, M., Abed, L., and Veraksa, A. (2008). Tandem affinity purification in Drosophila: the advantages of the GS-TAP system. Fly (Austin) *2*, 229–235.

Le Thomas, A., Rogers, A.K., Webster, A., Marinov, G.K., Liao, S.E., Perkins, E.M., Hur, J.K., Aravin, A.A., and Tóth, K.F. (2013). Piwi induces piRNA-guided transcriptional silencing and establishment of a repressive chromatin state. Genes Dev. *27*, 390–399.

Lin, H., and Spradling, A.C. (1997). A novel group of pumilio mutations affects the asymmetric division of germline stem cells in the Drosophila ovary. Development *124*, 2463–2476.

Ling, C., Zheng, Y., Yin, F., Yu, J., Huang, J., Hong, Y., Wu, S., and Pan, D. (2010). The apical transmembrane protein Crumbs functions as a tumor suppressor that regulates Hippo signaling by binding to Expanded. Proc. Natl. Acad. Sci. USA *107*, 10532–10537.

Losick, V.P., Morris, L.X., Fox, D.T., and Spradling, A. (2011). Drosophila stem cell niches: a decade of discovery suggests a unified view of stem cell regulation. Dev. Cell *21*, 159–171.

Lucas, E.P., Khanal, I., Gaspar, P., Fletcher, G.C., Polesello, C., Tapon, N., and Thompson, B.J. (2013). The Hippo pathway polarizes the actin cytoskeleton during collective migration of Drosophila border cells. J. Cell Biol. *201*, 875–885.

Lucchetta, E.M., and Ohlstein, B. (2012). The Drosophila midgut: a model for stem cell driven tissue regeneration. Wiley interdisciplinary reviews. Dev. Biol. *1*, 781–788.

Mitchell, N., Cranna, N., Richardson, H., and Quinn, L. (2008). The Ecdysone-inducible zinc-finger transcription factor Crol regulates Wg transcription and cell cycle progression in Drosophila. Development *135*, 2707–2716.

Mo, J.S., Park, H.W., and Guan, K.L. (2014). The Hippo signaling pathway in stem cell biology and cancer. EMBO Rep. *15*, 642–656.

modEncode Consortium, Roy, S., Ernst, J., Kharchenko, P.V., Kheradpour, P., Negre, N., Eaton, M.L., Landolin, J.M., Bristow, C.A., Ma, L., et al. (2010). Identification of functional elements and regulatory circuits by Drosophila modENCODE. Science *330*, 1787–1797.

Mohan, M., Herz, H.M., Smith, E.R., Zhang, Y., Jackson, J., Washburn, M.P., Florens, L., Eissenberg, J.C., and Shilatifard, A. (2011). The COMPASS family of H3K4 methylases in Drosophila. Mol. Cell. Biol. *31*, 4310–4318.

Nakada, D., Oguro, H., Levi, B.P., Ryan, N., Kitano, A., Saitoh, Y., Takeichi, M., Wendt, G.R., and Morrison, S.J. (2014). Oestrogen increases haematopoietic stem-cell self-renewal in females and during pregnancy. Nature *505*, 555–558.

Nijhout, H.F., and Grunert, L.W. (2002). Bombyxin is a growth factor for wing imaginal disks in Lepidoptera. Proc. Natl. Acad. Sci. USA *99*, 15446–15450.

Nijhout, H.F., Riddiford, L.M., Mirth, C., Shingleton, A.W., Suzuki, Y., and Callier, V. (2014). The developmental control of size in insects. Dev. Biol. *3*, 113–134.

Oh, H., and Irvine, K.D. (2011). Cooperative regulation of growth by Yorkie and Mad through bantam. Dev. Cell *20*, 109–122.

Oh, H., Reddy, B.V., and Irvine, K.D. (2009). Phosphorylation-independent repression of Yorkie in Fat-Hippo signaling. Dev. Biol. *335*, 188–197.

Oh, H., Slattery, M., Ma, L., White, K.P., Mann, R.S., and Irvine, K.D. (2014). Yorkie promotes transcription by recruiting a histone methyltransferase complex. Cell Rep. *8*, 449–459.

Pignoni, F., and Zipursky, S.L. (1997). Induction of Drosophila eye development by decapentaplegic. Development *124*, 271–278.

Reddien, P.W., Oviedo, N.J., Jennings, J.R., Jenkin, J.C., and Sánchez Alvarado, A. (2005). SMEDWI-2 is a PIWI-like protein that regulates planarian stem cells. Science *310*, 1327–1330.

Riddiford, L.M. (1993). Hormone receptors and the regulation of insect metamorphosis. Receptor *3*, 203–209.

Robinson, B.S., Huang, J., Hong, Y., and Moberg, K.H. (2010). Crumbs regulates Salvador/Warts/Hippo signaling in Drosophila via the FERM-domain protein Expanded. Curr. Biol. *20*, 582–590.

Ross, R.J., Weiner, M.M., and Lin, H. (2014). PIWI proteins and PIWI-interacting RNAs in the soma. Nature *505*, 353–359.

Salah, Z., and Aqeilan, R.I. (2011). WW domain interactions regulate the Hippo tumor suppressor pathway. Cell Death Dis. *2*, e172.

Sansores-Garcia, L., Bossuyt, W., Wada, K., Yonemura, S., Tao, C., Sasaki, H., and Halder, G. (2011). Modulating F-actin organization induces organ growth by affecting the Hippo pathway. EMBO J. *30*, 2325–2335.

Sato, K., Hayashi, Y., Ninomiya, Y., Shigenobu, S., Arita, K., Mukai, M., and Kobayashi, S. (2007). Maternal Nanos represses hid/skl-dependent apoptosis to maintain the germ line in Drosophila embryos. Proc. Natl. Acad. Sci. USA *104*, 7455–7460.

Sedkov, Y., Cho, E., Petruk, S., Cherbas, L., Smith, S.T., Jones, R.S., Cherbas, P., Canaani, E., Jaynes, J.B., and Mazo, A. (2003). Methylation at lysine 4 of histone H3 in ecdysone-dependent development of Drosophila. Nature *426*, 78–83.

Staley, B.K., and Irvine, K.D. (2012). Hippo signaling in Drosophila: recent advances and insights. Dev. Dyn. *241*, 3–15.

Strumane, K., Bonnomet, A., Stove, C., Vandenbroucke, R., Nawrocki-Raby, B., Bruyneel, E., Mareel, M., Birembaut, P., Berx, G., and van Roy, F. (2006). E-cadherin regulates human Nanos1, which interacts with p120ctn and induces tumor cell migration and invasion. Cancer Res. *66*, 10007–10015.

Sun, G., and Irvine, K.D. (2011). Regulation of Hippo signaling by Jun kinase signaling during compensatory cell proliferation and regeneration, and in neoplastic tumors. Dev. Biol. *350*, 139–151.

Thomas, H.E., Stunnenberg, H.G., and Stewart, A.F. (1993). Heterodimerization of the Drosophila ecdysone receptor with retinoid X receptor and ultraspiracle. Nature *362*, 471–475.

Tsai, C.C., Kao, H.Y., Yao, T.P., McKeown, M., and Evans, R.M. (1999). SMRTER, a Drosophila nuclear receptor coregulator, reveals that EcR-mediated repression is critical for development. Mol. Cell *4*, 175–186.

Turkel, N., Sahota, V.K., Bolden, J.E., Goulding, K.R., Doggett, K., Willoughby, L.F., Blanco, E., Martin-Blanco, E., Corominas, M., Ellul, J., et al. (2013). The BTB-zinc finger transcription factor abrupt acts as an epithelial oncogene in Drosophila melanogaster through maintaining a progenitor-like cell state. PLoS Genet. *9*, e1003627.

Yan, J., Tsai, S.Y., and Tsai, M.J. (2006). SRC-3/AIB1: transcriptional coactivator in oncogenesis. Acta Pharmacol. Sin. *27*, 387–394.

Yang, Y., Xu, S., Xia, L., Wang, J., Wen, S., Jin, P., and Chen, D. (2009). The bantam microRNA is associated with Drosophila fragile X mental retardation protein and regulates the fate of germline stem cells. PLoS Genet. *5*, e1000444.

Yao, T.P., Segraves, W.A., Oro, A.E., McKeown, M., and Evans, R.M. (1992). Drosophila ultraspiracle modulates ecdysone receptor function via heterodimer formation. Cell *71*, 63–72.